CrystEngComm

Accepted Manuscript

ROYAL SOCIETY OF CHEMISTRY

www.rsc.org/crystengcomm

Journal Name

RSCPublishing

ARTICLE

Polyrotaxane-like metal-organic framework showing luminescent sensing of Eu^{3+} cation and proton conductivity

Cite this: DOI: 10.1039/x0xx00000x

Received 00th January 2012,
Accepted 00th January 2012

DOI: 10.1039/x0xx00000x

www.rsc.org/

Bai-Qiao Song, Xin-Long Wang,* Guang-Sheng Yang, Hai-Ning Wang, Jun Liang, Kui-Zhan Shao and Zhong-Min Su*

A novel microporous metal-organic framework (MOF), namely $\{[Cd_2L_3(DMF)(NO_3)]\cdot 2DMF\cdot 3H_2O\}_n$ (**1**), where L = 1,3-bis(4-carboxyphenyl)imidazolium chloride, was prepared via a hydrothermal process. The structure of **1** shows the first example of 6-fold polyrotaxane-like interpenetration combined with interdigitation which extends the structure into three-dimensional framework, and exhibits reversible and irreversible guest-dependent structural conversion; Because of the 1D channels running along the b axis, **1** can serve as a host to encapsulate and sensitize Eu^{3+} cation in water. Moreover, the framework also shows a proton conductivity of over 10^{-5} S cm^{-1} at 298 K and 98% relative humidity due to the methylene hydrogens of the imidazolium moiety are highly acidic and aligned inside the channels which will enhance the proton conductivity.

Introduction

Entanglements are common in biology as seen in catenanes, rotaxanes and molecular knots,[1] and have captivated much attention due to their aesthetic and often complicated architectures and topologies.[2] Among these, Polyrotaxane,[3] as an intriguing branch of the entanglement system, which can be described as the extended periodic version of rotaxane motifs, have received considerable attentions for their mechanical links and potential applications in molecular machines or switches.[4] Since the pioneering work by Sauvage and Stoddart, admirable synthetic strategies initiated by Kim and Robson et al. have been developed to assemble rotaxanes (or pseudorotaxanes) into polyrotaxanes with highly ordered structures in the solid state, to lead a new field of polyrotaxane metal-organic frameworks (PMOFs).[3] Usually, as mentioned by Robson, Batten, Yang and Ma, in order to access the goal of polyrotaxane-like arrays the basic design requirement is the construction of a molecule unit with loops, and insertion of a linear rod through those loops.[3,4d] Based on this requirement, we think long rigid V-shaped ligand with two aromatic carboxylates at the terminal and an imidazolium group in the middle is a good candidate for the construction of polyrotaxane-like motif. First, the V-shaped structural character is beneficial for the formation of a loop and the ligand can also act as a rod; Second, the highly acidic methylene hydrogens of the imidazolium moiety from the rod can form hydrogen bonds with the oxygens on the loops; Third, the imidazolium moiety is electropositive which can produce ion-dipole interactions between the imidazolium N-atom on the rod and the oxygens on the loops. The hydrogen bonds and ion-dipole interactions have been proven to be crucial factors to hold the loop and rod together to form a pseudorotaxanes or rotaxane.[3]

Lanthanide ions have long been used as the key elements for a wide range of applications and technologies.[5] However, It is well-known that the luminescences of lanthanide cations have low molar absorptivity and that the f–f transitions are spin- and parity- forbidden.[6] As a result, these transitions have low absorption coefficients, making the direct excitation of the metals very inefficient. A "sensitization" process also known as the "antenna effect" has been developed to overcome this problem.[7] Metal–organic frameworks (MOFs) have several advantages that render them useful for sensitizing lanthanide cations. MOFs possess highly regular channel structures and controlled pore sizes in which a large number of chromophoric sensitizers and lanthanide cations can be incorporated. This inherent characteristic of MOFs can make each unit volume emit a large number of photons which will be helpful for the enhancement of the detection sensitivity.[8] The photoluminescence properties of lanthanide cations can be modulated and optimized by tailoring the MOF structures.[9] More importantly, MOFs provide a rigid scaffold that can serve to protect lanthanide cations from solvent quenching. Recently, An et al. prepared a series of lanthanide ions doped MOFs Ln^{3+}@bio-MOF-1 (Ln^{3+}=Tb^{3+}, Sm^{3+}, Eu^{3+}, or Yb^{3+}) from the

as-synthesized bio-MOF-1.[10] When excited at 365 nm, the doped MOFs emitted their distinctive colors, which are readily observed with the naked eye. Their results indicated a MOF can serve as both a host and an antenna for protecting and sensitizing extra-framework lanthanide cations emitting in the visible and NIR that are encapsulated within the MOF pores.

Although some fascinating polyrotaxane-like MOFs have been well documented in the literatures,[4,5] their potential applications still remain largely unexplored. Construction multifunctional MOFs with intriguing structural topologies and various potential applications remains challenging and more and more attention has been fixed on this topic.[11] In this paper, we report an unique polyrotaxane-like MOF $\{[Cd_2L_3(DMF)(NO_3)]\cdot 2DMF\cdot 3H_2O\}_n$ (**1**) ($H_2L^+Cl^-$ = 1,3-bis(4-carboxyphenyl)imidazolium chloride), which exhibits unique structural features combining interpenetration and interdigitation with intralayer porosity based on a 2D polyrotaxane-like framework. Furthermore, compound **1** shows multifunctionality: selectively luminescent sensing of Eu^{3+} cation in an aqueous environment and proton conductivity.

Experimental section

Materials and instruments

Chemicals were purchased from commercial sources and used without further purification. Powder X-ray diffraction (PXRD) was carried out with an X-ray diffractometer of Rigaku, Rint 2000. The C, H, and N elemental analyses were conducted on a Perkin-Elmer 240C elemental analyzer. The FT-IR spectra were recorded from KBr pellets in the range 4000-400 cm^{-1} on a Mattson Alpha-Centauri spectrometer. Thermogravimetric analyses (TGA) were carried out on a Perkin-Elmer TG-7 analyzer heated from room temperature to 800 ^oC at a ramp rate of 5 °C/min under nitrogen. The photoluminescence spectra were measured on a Perkin-Elmer FLS-920 spectrometer. ICP was measured by ICP-9000(N+M) (USA Thermo Jarrell-Ash Corp). Proton conductivity was measured on the powdered crystalline samples with 1.0-1.2 mm in thickness and 11.0 mm in diameter under a pressure of 12–14 MPa. Ac impedance spectroscopy measurement was performed on a chi660d (Shanghai Chenhua) electrochemical impedance analyzer with copper electrodes (the purity of Cu is more than 99.8 %) over the frequency range from 10^5–1 Hz. The conductivity was calculated as $\sigma = (1/R)(h/S)$, where R is the resistance, h is the thickness, and S is the area of the tablet. The contributions for the resistance R by the proton conductivity were estimated using the Nyquist plots.

Synthesis of $[Cd_2L_3(DMF)(NO_3)]\cdot 2DMF\cdot 3H_2O$ (1)

The ligand 1,3-bis(4-carboxyphenyl)imidazolium chloride ($H_2L^+Cl^-$) was prepared following the method as described in the literature.[12] A solid mixture of $H_2L^+Cl^-$ (30 mg, 0.4 mmol), $Cd(NO_3)_2\cdot 4H_2O$ (120 mg, 0.1 mmol) was dissolved in DMF (3 ml) in a 8ml vial. The mixture was heated in an isotherm oven at 120 °C for 72 h resulting in colorless crystals, which were isolated by washing with DMF and hexane. The sample was dried in air at room temperature overnight. Yield: 51% based on 1 mol of $H_2L^+Cl^-$. Elemental analyses calcd (%) for $C_{60}H_{60}Cd_2N_{10}O_{21}$ (1481.98): C, 48.58; H, 4.05; N, 9.45; Found C, 48.50; H, 4.12; N, 9.46. IR (KBr pellet,cm^{-1}): 3421 (m), 3087 (m), 1658 (w), 1610 (w), 1548 (w), 1387 (w), 1253 (m), 1100 (s), 1064 (s), 1014 (s), 953 (s), 855(m), 782 (m), 728 (s), 695 (s), 659 (s), 621 (s), 526 (s).

Desolvated sample (1b): Compound **1** was soaked in MeOH at room temperature for 72 h. The MeOH exchanged sample **1a** was obtained after being dried in air for 24 h. Heating the MeOH exchanged sample at 100 °C under vacuum for 12 h produced the desolvated sample **1b**.

Resolvated sample: The activated sample of **1b** was immersed in DMF at 60 °C for 24 h to give the resolvated sample. The same process was performed to resolvate the MeOH exchanged sample **1a**.

X-ray crystallography study

Single-crystal X-ray diffraction data were recorded on a Bruker Apex CCD diffractometer with graphite-monochromated MoKα radiation (λ = 0.71069 Å) at 293K. Absorption corrections were applied using multi-scan technique. All the structures were solved by Direct Method of SHELXS-97[13] and refined by full-matrix least-squares techniques using the SHELXL-97 program[14] within WINGX.[15] Non-hydrogen atoms were refined with anisotropic temperature parameters except for six disorder atoms which were refined with isotropic. Because guest solvent molecules (DMF and H_2O) in the frameworks of **1** were highly disordered, the diffused electron densities resulting from them were removed by the SQUEEZE routine in PLATON[16] and the platon.sqf files were attached to the CIF files. The electron number in the void obtained from the platon.sqf files have been used to calculate the guest solvent molecules crystallizing in the pore of **1**. These molecules are further estimated by TGA analysis combining with element

Table 1 Crystal data and structure refinements for **1**

Compound reference	**1**
Chemical formula	$C_{60}H_{60}Cd_2N_{10}O_{21}$
Formula Mass	1481.98
Crystal system	Monoclinic
a/Å	47.182(5)
b/Å	9.857(5)
c/Å	32.787(5)
α/°	90
β/°	101.008(5)
γ/°	90
Unit cell volume/Å^3	14968(8)
Temperature/K	293(2)
Space group	*C*2/*c*
No. of formula units per unit cell, *Z*	8
No. of reflections measured	37516
No. of independent reflections	13117
R_{int}	0.0450
Final R_1 values ($I > 2\sigma(I)$)	0.0459
Final $wR(F^2)$ values ($I > 2\sigma(I)$)	0.1196
Final R_1 values (all data)	0.0706
Final $wR(F^2)$ values (all data)	0.1283
Goodness of fit on F^2	0.963

analysis, and the results were introduced to the CIF files. The detailed crystallographic data and structure refinement parameters for **1** are summarized in Table 1. Selected bond lengths and angles for complexes **1** are given in Table S1.

Results and discussion

Structural descriptions

1 was obtained as colourless needle crystal from a reaction of 1,3-bis(4-carboxyphenyl) imidazolium chloride ($H_2L^+Cl^-$), and $Cd(NO_3)_2{\cdot}6H_2O$ in DMF under solvothermal conditions in moderate yields. Single crystal X-ray diffraction analysis reveals that **1** crystallizes in the monoclinic space group C2/c. There are two crystallographically independent Cd centers and three V-shaped ligands with different coordination modes in the asymmetry unit (Fig. 1). Cd1 coordinates with three bidentate carboxylate groups from three ligands and one bidentate NO_3^-, while Cd2 coordinates with two bidentate carboxylate groups from two ligands and one monodentate carboxylate group from one ligand and a DMF molecule. Simply, every Cd center can be considered as a three connected node and six Cd(II) ions are linked by six L^- to form a large $[Cd_6L_6]$ 6-membered ring with the dimensions of the longest diagonal being 27.94 Å, 35.28 Å and 39.61 Å. Two contiguous $[Cd_6L_6]$ rings share two Cd ions and one L^- ligand to form a loop-like chain (Fig. 2).[17] All the loop-like chains are parallel arrangement and the distance between two parallel chains is 29.57 Å. The adjacent chains are bridged by a L^- ligand to generate a 2D infinite bow-shaped (6,3) layer (Fig. 3a, S1, ESI†), Although the (6,3) net is one of the most common topologies in 2D coordination polymers, the bow-shaped (6,3) layer is rare. In this case, the 6-membered ring is so large, which permits the other two identical layers to interpenetrate it in a parallel fashion, resulting in a 3-fold parallel interpenetrating network (Fig. 3b). Compared with the single (6,3) layer, the distance between adjacent parallel loop-like chains in the 3-fold interpenetrating 2D structure has reduced to 9.86 Å, which means there still has enough space to accommodate another loop-like chain in a parallel fashion. Nature abhors a vacuum. In order to minimize the big voids and stabilize the framework, the potential voids formed by one 3-fold interpenetrating 2D network show incorporation of another identical network in a top-to-top fashion, thus generating a new 2D 6-fold interpenetrating network (Fig. 3c). In this new 2D network, one 6-membered ring from one 3-fold interpenetrating network is threaded through simultaneously by two ligand rods from two bow-shaped (6,3) layers belong to the identical 3-fold interpenetrating network and three ligand rods from three bow-shaped (6,3) layers belong to another 3-fold interpenetrating network (Fig. 3d). Actually, if we consider each Cd_6L_6 unit as a loop and one ligand as a single rod, then the entanglement can be seen as a first type of polyrotaxane-like motif by one ring with ten stoppers rather than the reported ones by one ring with two or four stoppers.[4d] Closer inspection reveals that the hydrogen bonds between the 6-membered ring and one ligand rod passing through it induce the rod-to-ring rotaxane interactions (Fig. S2, ESI†).

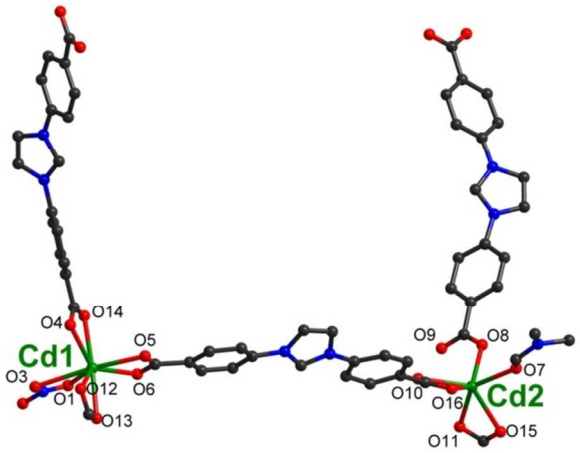

Fig. 1 The coordination environment of Cd in **1.** Green, blue, black, and red spheres represent Cd, N, C, O, respectively.

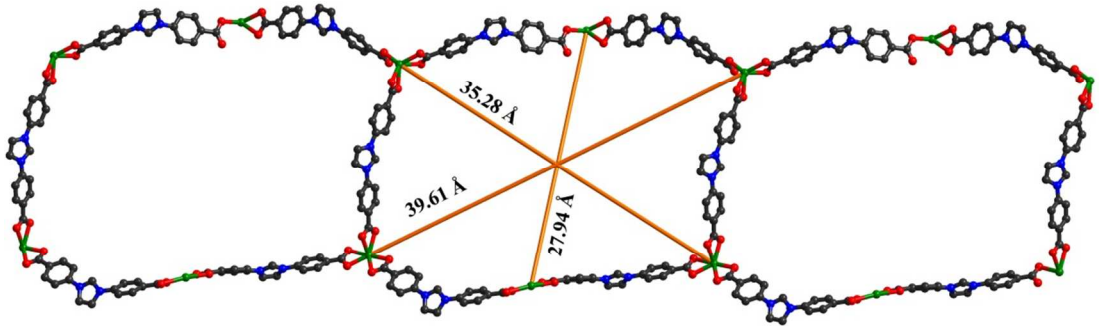

Fig. 2 The loop-like chain formed by $[Cd_6L_6]$ 6-membered rings with the corresponding sizes in **1**.

Journal Name RSCPublishing

ARTICLE

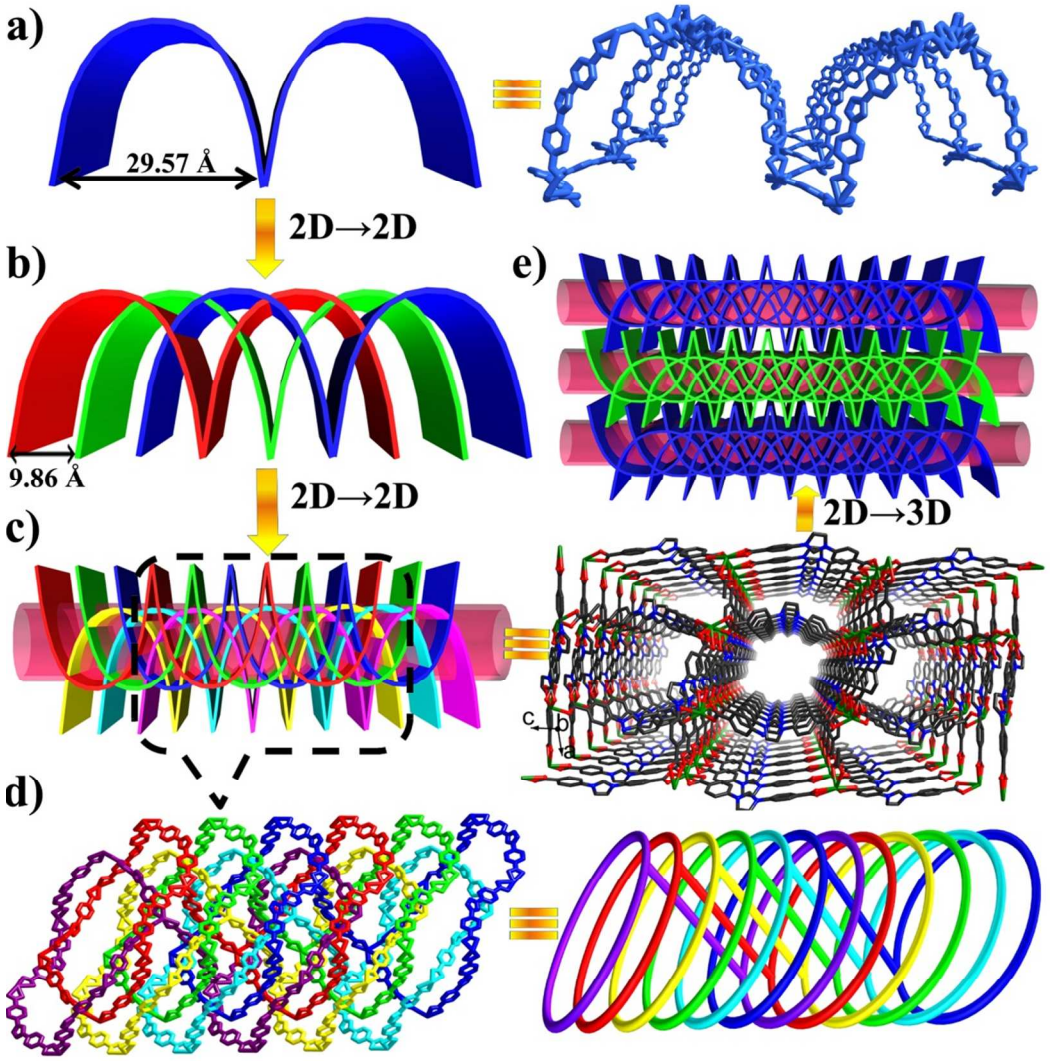

Fig. 3 a) View of the bow-shaped (6,3) layer. b) View of the 2D→2D parallel interpenetration. c) 2D→2D 6-fold polyrotaxane-like interpenetration with intralayer 1D channels. d) One 6-membered ring unit is threaded through by five armed rods of the adjacent layers. e) Schematic representation of the 2D→3D interdigitated array. Light red tubes represent the intralayer 1D channels. Hydrogen atoms, NO_3^-, DMF and H_2O molecules are omitted for clarity.

Interpenetration phenomena are ubiquitous during the self-assembly process, but the 2D 6-fold interpenetrating net is scare. To the best of our knowledge, this is the first example of 2D 6-fold polyrotaxane-like interpenetrating network. Further study into the nature of the intricate architecture in **1** showed that the 6-fold polyrotaxane-like 2D layer display an interesting sawtooth-like arrangement in which each loop-like chain act as a 'tooth' (Fig. 3c). The adjacent layers are arranged in an interdigitated array to extend into 3D structure where one 'tooth' from one layer inserts into the void between two adjacent 'teeth' on the another layer (Fig. 3e).[18] The hydrogen bonds between the highly acidic methylene hydrogen of the imidazolium moiety and oxygen atoms (C-H···O = 2.974-3.267 Å) further stabilize the structure (Fig. S3). Interestingly, even in the presence of mutual interpenetration and interdigitation, there are 1D channels running along the b axis in **1**, with a largest dimension of ca. 11.3 and 11.0 Å, possessing corresponding volume of 38.4% using PLATON,[16] which are occupied by DMF and H_2O molecules (Fig. 3c, S4).

In contrast with the common porous architectures, the special 6-fold polyrotaxane-like interpenetrated structure and interdigitated packing mode may greatly increase the dynamic nature of the framework. The PXRD pattern of the MeOH exchanged sample (**1a**) shows very different from that of **1** (Fig. S5, ESI†). When **1a** was immersed in DMF at 60 °C for 48 h, a reversible structural transformation appeared from **1a** to **1**. The desolvated sample (**1b**) was generated after heating **1a** at 80 °C under vacuum for 6 h. As checked by the PXRD data, the phase of **1b** is identical to that of **1a**. Similarly, when **1b** was placed in DMF at 60 °C for 24 h, **1** was recovered. However, when **1**, **1a** or **1b** was immersed in water at room temperature or at 100 °C for three days, an irreversible structural transformation from **1**, **1a**, or **1b** to **1c** occurred (Fig. S6, ESI†). We suppose two reasons are responsible for the structure conversion: the sliding of interpenetrated networks[19] with the aid of hydrogen bonds and the possible movement of the 2D interdigitated structures in addition to local bond lengths and angles shift or change during the guest accommodation and release (Fig. S7, ESI†).[20]

luminescent sensing of Eu^{3+}

Because of the highly regular channel structures and controlled pore sizes, the MOFs can also serve as rigid/flexible hosts for the encapsulation of the guest luminescent species such as lanthanide ions and fluorescent dyes.[21] MOFs encapsulating and sensitizing lanthanide ions in an aqueous environment is a versatile strategy for preparing luminescent materials that may have applications in biological systems.[22] To introduce lanthanide ions into **1,** fresh samples of **1** were soaked in 0.3 mol L^{-1} DMF solutions of nitrate salts of Eu^{3+}, Sm^{3+}, Tb^{3+} and Dy^{3+} for 120 h. XPS, ICP and TGA curves were used to analyse the Ln^{3+}-treated materials, the results revealed no Sm^{3+}, Tb^{3+} and Dy^{3+} lanthanide cations incorporation into **1** except for Eu^{3+} cation (Fig. S8, S9, Table S2, ESI†). Surprisingly, the Eu^{3+} doped material **Eu^{3+}@1 (1d)** shows structure transformation while the other Ln^{3+} treated samples still keep their crystalline integrity during the whole treatments, as demonstrated by its PXRD profiles (Fig. S10, ESI†). Meanwhile, the IR spectrum of **Eu@1** shows scarcely any free DMF and H_2O molecules in it (Fig. S4). The phase of **1d** is almost identical to that of **1a** (**1b**) except for a small shift from some peaks to lower angle. The photoluminescence emission spectrum recorded for **1d** in DMF indicated the host structure can sensitize the visible emitting of Eu^{3+} lanthanide cation in an organic solvent (Fig. S12, ESI†). Encouraged by this result, **1d** was soaked in water in a quartz cuvette for 48 h, when excited with a standard laboratory UV lamp (365 nm), **1d** in water emitted its distinctive red color, which was readily observed by the naked eye as a qualitative indication of Eu^{3+} sensitization (Fig. 4). Importantly, after all the measurements in water, **1d** still retained its crystallinity, as evidenced by its PXRD patterns. As mentioned above, when **1a (1b)** was soaked in water, it changes structure to **1c**, but when Eu^{3+} encapsulated sample **1d** was soaked in water, it retained its crystallinity (Fig. S11, ESI†), which means the incorporation of the Eu^{3+} ions in **1** can induce the structure transformation and enhance the stability of the structure in water.

Fig. 4 presents the photoluminescence emission spectrum recorded for Eu^{3+} doped sample in water which shows typical Eu^{3+} red emissions and exhibits well-resolved peaks centered at ~579, 592, 616, 653, and 702 nm, corresponding to the transitions from the metal centered $^5D_0$ excited state to the ^7F_J (J =0−4) ground state multiplet with the hypersensitive $^5D_0 \rightarrow {}^7F_2$ transition dominating the spectra which implies a red emission light.[23] The emission in the range of 400–500 nm corresponding to the frameworks is much weaker than that of **1**. For Eu^{3+} doped sample, the intraligand emission of the frameworks may be suppressed by the energy transfer. Therefore, we can conclude that the changed structure effectively serve as an antenna for sensitizing the visible emitting Eu^{3+} cation in organic solvent and water.

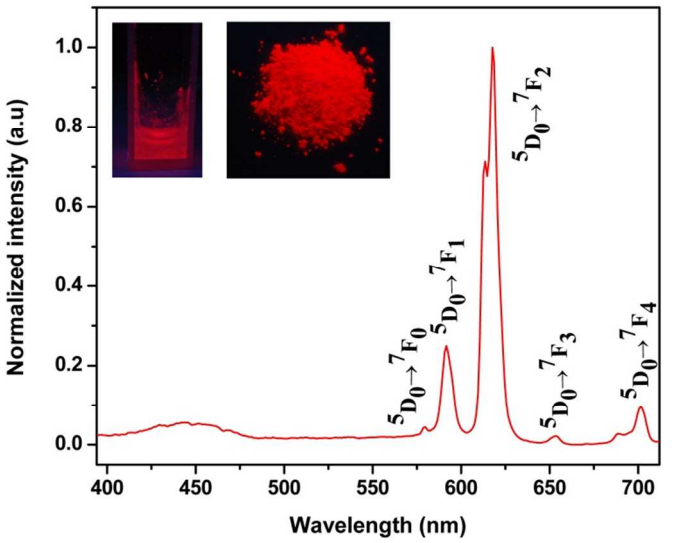

Fig. 4 Photoluminescence of **Eu^{3+}@1** in water. Inset: photographs showing **Eu^{3+}@1** in water as well as crystals of **Eu^{3+}@1** after soaked in water for 48 h illuminating with 365 nm laboratory UV light.

proton conductivity

Proton conductivity in solid-state materials plays important roles for their potential applications in electrochemical devices, fuel cells and in the field of better understanding transport dynamics.[24] There have two reasons spurring us to investigate the proton conductivity of **1**, first, the acidic methylene protons of some imidazolium moieties are aligned along the channels which can act as proton carriers to enhance the proton conductivity (Fig. 3c).[12a,25] Second, the space between the microporous 2D layers can accommodate some slovent molecules, such as water, which will be help for the proton conductivity.[25c, 26] The proton conductivities of **1** at 298 K in the relative humidity (RH) of approximately 40% to 98% were evaluated by the AC impedance spectroscopy method by using a compacted pellet of the powdered crystalline sample (Fig. S13, ESI†). The humidity dependence of proton conductivities of MOF **1** are shown in Fig. 5a, increasing trend in conductivity

is observed as the relative humidity is increased. The proton conductivity of **1** is 1.51×10^{-8} S cm^{-1} at 298 K, about 40% RH and reaches 3.25×10^{-5} S cm^{-1} at 298 K, about 98% RH, suggesting that water molecules play an important role in the proton conductivity. The temperature dependent study is also given in Fig. 5b. Arrhenius plot shows a linear behaviour and the derived activation energy (Ea) for the conduction process was estimated to be 0.38 eV, this reported activation energy is located within the range typically attributed to a Grotthuss transfer mechanism via water molecules (0.1−0.4 eV).[27]

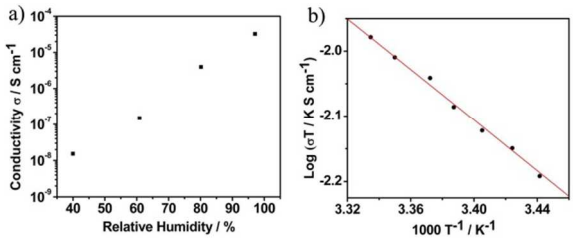

Fig 5 a) Proton conductivity dependence on humidity at 298 K. b) Arrhenius plots of the conductivity of **1**.

Conclusions

In summary, a 2D flexible microporous polyrotaxane-like MOF have been successfully synthesized based on Cd cations and bicarboxylate Imidazolium salts ligand. The crystal material displays reversible and irreversible phase transformation induced by different guests. Especially, it can selectively encapsulate and sensitize of the visible-emitting Eu^{3+} cation in water. The incorporation of Eu^{3+} ions can induce the structure transformation and enhance the stability of the structure in water. The framework also shows a proton conductivity of over 10^{-5} S cm^{-1} at 298 K and 98% relative humidity.

Acknowledgements

This work was financially supported by the NSFC of China (Nos. 21001022, 21171033, 21131001, 21222105, 21071124, 21173189), PhD Station Foundation of Ministry of Education (20100043110003), The Foundation for Author of National Excellent Doctoral Dissertation of P. R. China (FANEDD) (No. 201022), The Science and Technology Development Planning of Jilin Province (201001169, 20111803). We thank three referees for their helpful comments.

Notes and references

Institute of Functional Material Chemistry；Key Laboratory of Polyoxometalate Science of Ministry of Education, Northeast Normal University, Changchun, 130024 Jilin, People's Republic of China. E-mail: wangxl824@nenu.edu.cn, zmsu@nenu.edu.cn; Fax: + 86 431-85684009; Tel: + 86 431-85099108

† Electronic Supplementary Information (ESI) available: Schemes, figures and CIF files giving additional structural figures, PXRD, TGA, IR and crystallographic data (CCDC 969162), and details of experiments. See DOI: 10.1039/b000000x/

1 S. R. Batten and R. Robson, in *Molecular Catenanes, Rotaxanes and Knots, A Journey Through the World of Molecular Topology*, eds. J.-P. Sauvage and C. Dietrich-Buchecker, Wiley-VCH, Weinheim, 1999.

2 (a) X. H. Bu, M. L. Tong, H. C. Chang, S. Kitagawa and S. R. Batten, *Angew. Chem. Int. Ed.*, 2004, **43**, 192-195; (b) S. A. Bourne, J. Lu, B. Moulton and M. J. Zaworotko, *Chem. Commun.*, 2001, 861-862; (c) V. Blatov, L. Carlucci, G. Ciani and D. Proserpio, *CrystEngComm*, 2004, **6**, 377-395; (d) L. Carlucci, G. Ciani and D. M. Proserpio, *CrystEngComm*, 2003, **5**, 269-279; (e) C. Janiak, *Dalton Transactions*, 2003, 2781-2804; (f) X. L. Wang, C. Qin, E. B. Wang, L. Xu, Z. M. Su and C. W. Hu, *Angew. Chem. Int. Ed.*, 2004, **116**, 5146-5150; (g) X. L. Wang, C. Qin, E. B. Wang and Z. M. Su, *Chem.-Eur. J.*, 2006, **12**, 2680-2691.

3 (a) L. Carlucci, G. Ciani and D. M. Proserpio, *Coord. Chem. Rev.*, 2003, **246**, 247-289; (b) J. Yang, J.-F. Ma and S. R. Batten, *Chem. Commun.*, 2012, **48**, 7899-7912; (c) S. R. Batten and R. Robson, *Angew. Chem. Int. Ed.*, 1998, **37**, 1460-1494; (d) S. R. Batten, *CrystEngComm*, 2001, **3**, 67-72;eK. Kim, *Chem. Soc. Rev.*, 2002, **31**, 96-107; (f) S. J. Loeb, *Chem. Commun.*, 2005, 1511-1518.

4 (a) J. Liang, X.-L. Wang, Y.-Q. Jiao, C. Qin, K.-Z. Shao, Z.-M. Su and Q.-Y. Wu, *Chem. Commun.*, 2013, **49**, 8555-8557; (b) C. Qin, X.-L. Wang, E.-B. Wang and Z.-M. Su, *Inorg. Chem.*, 2008, **47**, 5555-5557; (c) X.-L. Wang, C. Qin, E.-B. Wang and Z.-M. Su, *Chem. Commun.*, 2007, 4245-4247; (d) H. Wu, H.-Y. Liu, Y.-Y. Liu, J. Yang, B. Liu and J.-F. Ma, *Chem. Commun.*, 2011, **47**, 1818-1820.

5 (a) M. L. Cable, D. J. Levine, J. P. Kirby, H. B. Gray and A. Ponce, in *Adv. Inorg. Chem.*, eds. E. Rudi van and S. Grażyna, Academic Press, 2011, pp. 1-45; (b) S. V. Eliseeva and J.-C. G. Bunzli, *New J. Chem.*, 2011, **35**, 1165-1176; (c) S. J. Butler and D. Parker, *Chem. Soc. Rev.*, 2013, **42**, 1652-1666; (d) J.-C. G. Bunzli and S. V. Eliseeva, *Chemical Science*, 2013, **4**, 1939-1949; (e) J. Heine and K. Muller-Buschbaum, *Chem. Soc. Rev.*, 2013, **42**, 9232-9242; (f) M. D. Allendorf, C. A. Bauer, R. K. Bhakta and R. J. T. Houk, *Chem. Soc. Rev.*, 2009, **38**, 1330-1352; (g) Y. Cui, Y. Yue, G. Qian and B. Chen, *Chem. Rev.*, 2011, **112**, 1126-1162; (h) J. Rocha, L. D. Carlos, F. A. A. Paz and D. Ananias, *Chem. Soc. Rev.*, 2011, **40**, 926-940.

6 G. Blasse and B. Grabmaier, *Luminescent materials*, Springer, 1994.

7 (a) J. C. G. Bünzli and S. V. Eliseeva, in *Comprehensive Inorganic Chemistry II (Second Edition)*, eds. J. Reedijk and K. Poeppelmeier, Elsevier, Amsterdam, 2013, pp. 339-398; (b) E. G. Moore, A. P. S. Samuel and K. N. Raymond, *Acc. Chem. Res.*, 2009, **42**, 542-552.

8 C.-Y. Sun, X.-L. Wang, X. Zhang, C. Qin, P. Li, Z.-M. Su, D.-X. Zhu, G.-G. Shan, K.-Z. Shao, H. Wu and J. Li, *Nat Commun*, 2013, **4**, 2717.

9 (a) K. A. White, D. A. Chengelis, M. Zeller, S. J. Geib, J. Szakos, S. Petoud and N. L. Rosi, *Chem. Commun.*, 2009, 4506-4508; (b) K. A. White, D. A. Chengelis, K. A. Gogick, J. Stehman, N. L. Rosi and S. Petoud, *J. Am. Chem. Soc.*, 2009, **131**, 18069-18071.

10 J. An, C. M. Shade, D. A. Chengelis-Czegan, S. Petoud and N. L. Rosi, *J. Am. Chem. Soc.*, 2011, **133**, 1220-1223.

11 (a) J. Cao, Y. Wang, C. Du and Z. Liu, *Chem. Commun.*, 2013; (b) H.-N. Wang, X. Meng, G.-S. Yang, X.-L. Wang, K.-Z. Shao, Z.-M. Su and C.-G. Wang, *Chem. Commun.*, 2011, **47**, 7128-7130; (c) L. Chen, K. Tan, Y.-Q. Lan, S.-L. Li, K.-Z. Shao and Z.-M. Su, *Chem. Commun.*, 2012, **48**, 5919-5921; (d) W.-W. He, S.-L. Li, G.-S. Yang,

Y.-Q. Lan, Z.-M. Su and Q. Fu, *Chem. Commun.*, 2012, **48**, 10001-10003.

12 (a) S. Sen, N. N. Nair, T. Yamada, H. Kitagawa and P. K. Bharadwaj, *J. Am. Chem. Soc.*, 2012, **134**, 19432-19437; (b) J. Y. Lee, J. M. Roberts, O. K. Farha, A. A. Sarjeant, K. A. Scheidt and J. T. Hupp, *Inorg. Chem.*, 2009, **48**, 9971-9973; (c) J. Chun, I. G. Jung, H. J. Kim, M. Park, M. S. Lah and S. U. Son, *Inorg. Chem.*, 2009, **48**, 6353-6355.

13 G. M. Sheldrick, *SHELXS-97: Program for X-ray crystal structure solution;*, University of Göttingen: Göttingen, Germany, 1997.

14 G. M. Sheldrick, *SHELXL-97: Program for X-ray Crystal Structure Refinement;* , University of Göttingen: Göttingen, Germany, 1997.

15 L. J. Farrugia, *WINGX: A Windows Program for Crystal Structure Analysis;* , University of Glasgow: Glasgow, UK, 1988.

16 A. Spek, *J. Appl. Crystallogr.*, 2003, **36**, 7-13.

17 H. Wu, B. Liu, J. Yang, H.-Y. Liu and J.-F. Ma, *CrystEngComm*, 2011, **13**, 3661-3664.

18 (a) T. Fukushima, S. Horike, H. Kobayashi, M. Tsujimoto, S. Isoda, M. L. Foo, Y. Kubota, M. Takata and S. Kitagawa, *J. Am. Chem. Soc.*, 2012, **134**, 13341-13347; (b) Z. Yin, Q.-X. Wang and M.-H. Zeng, *J. Am. Chem. Soc.*, 2012, **134**, 4857-4863.

19 B. Chen, C. Liang, J. Yang, D. S. Contreras, Y. L. Clancy, E. B. Lobkovsky, O. M. Yaghi and S. Dai, *Angew. Chem. Int. Ed.*, 2006, **118**, 1418-1421.

20 (a) P. Kanoo, G. Mostafa, R. Matsuda, S. Kitagawa and T. K. Maji, *Chem. Commun.*, 2011, **47**, 8106-8108; (b) E. Jeong, W. R. Lee, D. W. Ryu, Y. Kim, W. J. Phang, E. K. Koh and C. S. Hong, *Chem. Commun.*, 2013, **49**, 2329-2331.

21 J. Yu, Y. Cui, H. Xu, Y. Yang, Z. Wang, B. Chen and G. Qian, *Nat Commun*, 2013, **4**.

22 A. Foucault-Collet, K. A. Gogick, K. A. White, S. Villette, A. Pallier, G. Collet, C. Kieda, T. Li, S. J. Geib, N. L. Rosi and S. Petoud, *Proceedings of the National Academy of Sciences*, 2013, **110**, 17199-17204.

23 Y.-L. Gai, F.-L. Jiang, L. Chen, Y. Bu, K.-Z. Su, S. A. Al-Thabaiti and M.-C. Hong, *Inorg. Chem.*, 2013, **52**, 7658-7665.

24 (a) G. K. Shimizu, J. M. Taylor and S. Kim, *Science*, 2013, **341**, 354-355; (b) M. Yoon, K. Suh, S. Natarajan and K. Kim, *Angew. Chem. Int. Ed.*, 2013, **52**, 2688-2700; (c) T. Yamada, K. Otsubo, R. Makiura and H. Kitagawa, *Chem. Soc. Rev.*, 2013, **42**, 6655-6669; (d) S. Horike, D. Umeyama and S. Kitagawa, *Acc. Chem. Res.*, 2013;(e) X. Meng, X.-Z. Song, S.-Y. Song, G.-C. Yang, M. Zhu, Z.-M. Hao, S.-N. Zhao and H.-J. Zhang, *Chem. Commun.*, 2013, **49**, 8483-8485; (f) X. Liang, F. Zhang, W. Feng, X. Zou, C. Zhao, H. Na, C. Liu, F. Sun and G. Zhu, *Chemical Science*, 2013, **4**, 983-992; (g) C. Dey, T. Kundu and R. Banerjee, *Chem. Commun.*, 2012, **48**, 266-268.

25 (a) J. M. Taylor, R. K. Mah, I. L. Moudrakovski, C. I. Ratcliffe, R. Vaidhyanathan and G. K. H. Shimizu, *J. Am. Chem. Soc.*, 2010, **132**, 14055-14057; (b) A. Shigematsu, T. Yamada and H. Kitagawa, *J. Am. Chem. Soc.*, 2011, **133**, 2034-2036; (c) D. Umeyama, S. Horike, M. Inukai, T. Itakura and S. Kitagawa, *J. Am. Chem. Soc.*, 2012, **134**, 12780-12785; (d) S. Bureekaew, S. Horike, M. Higuchi, M. Mizuno, T. Kawamura, D. Tanaka, N. Yanai and S. Kitagawa, *Nat Mater*, 2009, **8**, 831-836; (e) J. A. Hurd, R. Vaidhyanathan, V. Thangadurai, C. I. Ratcliffe, I. L. Moudrakovski and G. K. H. Shimizu, *Nat Chem*, 2009, **1**, 705-710; (f) M. Sadakiyo, T. Yamada and H. Kitagawa, *J. Am. Chem. Soc.*, 2009, **131**, 9906-9907.

26 H. Ōkawa, M. Sadakiyo, T. Yamada, M. Maesato, M. Ohba and H. Kitagawa, *J. Am. Chem. Soc.*, 2013, **135**, 2256-2262.

27 P. Colomban, Proton Conductors: Solids, membranes and gels-materials and devices, Cambridge University Press, 1992.

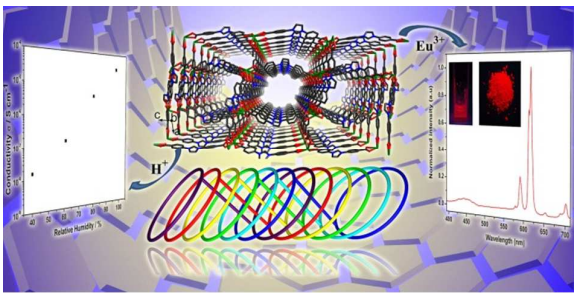

The first example of 6-fold polyrotaxane-like microporous interpenetrating network was prepared, showing luminescent sensing of Eu^{3+} cation and proton conductivity.